HHS Public Access

Author manuscript

Int Forum Allergy Rhinol. Author manuscript; available in PMC 2023 March 01.

Published in final edited form as:

Int Forum Allergy Rhinol. 2023 March ; 13(3): 230–241. doi:10.1002/alr.23073.

Chronic interleukin-13 expression in mouse olfactory mucosa results in regional aneuronal epithelium

Anirudh Saraswathula, MD, MS,

Melissa M. Liu, MD, PhD,

Heather Kulaga, MS,

Andrew P. Lane, MD

Department of Otolaryngology-Head and Neck Surgery, Johns Hopkins University School of Medicine, Baltimore, Maryland, USA

Abstract

Background: Olfactory dysfunction is highly associated with chronic rhinosinusitis with nasal polyps (CRSwNP), and the severity of loss has been linked with biomarkers of type 2 inflammation. The ability of dupilumab to rapidly improve the sense of smell prior to improvement in polyp size suggests a direct role of IL-4/IL-13 receptor signaling in the olfactory epithelium (OE).

Methods: We created a transgenic mouse model in which IL-13 is inducibly expressed specifically within the OE. Gene expression analysis and immunohistology were utilized to characterize the effect of IL-13 on the structure of the OE.

Results: After induction of olfactory IL-13 expression, there is a time-dependent loss of neurons from OE regions, accompanied by a modest inflammatory infiltrate. Horizontal basal cells undergo morphologic changes consistent with activation and demonstrate proliferation. Mucus production and increased expression of eotaxins is observed, with marked expression of Ym2 by sustentacular cells.

Discussion: Chronic IL-13 exposure has several effects on the OE that are likely to affect function. The neuronal loss is in keeping with other models of allergic type 2 nasal inflammation. Future studies are needed to correlate cellular and molecular alterations in olfactory cell populations with findings in human CRSwNP, as well as to assess olfactory function in behavioral model systems.

Keywords

inflammation; interleukin 13; olfactory loss; sustentacular cells

Correspondence: Andrew P. Lane MD, Department of Otolaryngology-Head and Neck Surgery, Johns Hopkins Outpatient Center, 6th Floor, 601 North Caroline Street, Baltimore, MD 21287-0910, USA. alane3@jhmi.edu.

CONFLICT OF INTEREST

None.

To be presented at the American Rhinologic Society Spring Meeting, April 28, 2022, Dallas, TX, USA.

1 | INTRODUCTION

Olfactory loss has attracted significant new interest in recent years, particularly with the strong association of the condition with SARS-CoV-2 infection. While trauma and upper respiratory infections (URIs) are common etiologies of anosmia, chronic rhinosinusitis (CRS) is its leading cause worldwide,[1] with over 50% of patients with CRS with nasal polyposis (CRSwNP) reporting anosmia on presentation.[2]

The mechanism for anosmia in CRS is likely at least partially obstructive in nature. In the basic mechanism of olfaction, odorants are inspired into the upper nasal cavity and enter the olfactory cleft. This region, bordered superiorly by the cribriform plate and medially and laterally by the nasal septum and the middle and superior turbinates, respectively, is lined with olfactory neuroepithelium covered by a layer of olfactory mucus produced by Bowman's glands. This microenvironment of this mucus, with its odorant binding proteins and specific ionic composition, promotes transduction of olfactory signaling. Diffusing into this mucus, odorants are then detected by the cilia of olfactory receptor neurons, which project above the apical mucosal surface formed by a specialized epithelial cell type called sustentacular cells that comprise a barrier and provide functional and physical support to the neurons.[3] In CRS, and particularly in CRSwNP, mechanical obstruction from edema and inflammation as well as disruption of mucociliary clearance impairs delivery of odorants to the olfactory neuroepithelium.[4]

Obstruction is not the only mechanism at play in inflammation-associated olfactory dysfunction, however, as neuroepithelial inflammation and damage also play an important role. Histopathologic studies of the olfactory mucosa in CRS patients reveal infiltration of lymphocytes, macrophages, and eosinophils throughout the olfactory epithelium (OE) as well as squamous metaplasia and epithelial erosion.[1,5,6] Additionally, type 2 cytokines, most notably interleukin-5(IL-5) and IL-13, have been found to be elevated in the intraoperatively collected olfactory cleft mucus of CRS patients, and even higher in a CRSwNP subset.[7–9]

The loss of the sense of smell in CRS can often be improved temporarily with systemic corticosteroids, although it is unclear whether the mechanism is indirect through a generalized reduction of inflammation or through direct action on olfactory cells.[10] Dupilumab is a monoclonal antibody targeting the receptor for IL-4 and IL-13 that has relatively recently been demonstrated to be safe and highly effective in treating CRSwNP inflammation.[11,12] In addition to reducing nasal polyp size and improving symptoms, dupilumab has been shown to significantly improve the sense of smell in CRSwNP patients.[13] Other biologics, mepolizumab and benralizumab (both anti-IL-5 monoclonal antibodies), and omalizumab (anti-IgE) have also been reported to result in improvement in anosmia caused by CRSwNP, although to a lesser extent.[14–16] Notably, smell function gains are noted to precede significant change in polyp size, suggesting a direct role of IL-4/IL-13 receptor signaling in this pathophysiology. Currently, however, there is a dearth of experimental evidence surrounding mechanisms of IL-4 and IL-13 action in the olfactory neuroepithelium.

In this study, we sought to better characterize the relationship between type 2 inflammation and olfactory dysfunction. Using a transgenic mouse model with temporally controlled olfactory-specific gene expression, we explored the impact of chronic IL-13 on the OE, utilizing molecular and immunohistologic techniques.

2 | METHODS

2.1 | Mice

The Rosa26-CAGs-LSL-rtTA3 knock-in mouse line was purchased from Jackson Laboratory (stock no. 029617, Bar Harbor, ME). The transgene TRE-Tight-IL-13 strain[17] and the OMP-Cre strain (Jackson Laboratory, stock no. 006668) were crossed with the Rosa26-CAGs-LSL-rtTA3 knock-in mouse line. Based on the Tet-on genetic system, 3–6-week-old mice were treated with 2 g/kg doxycycline food for 3 weeks to induce IL-13 expression specifically by the mature olfactory sensory neurons (OSNs). This time point was chosen to be in the range of published murine model studies of olfactory epithelial inflammation. Mice utilized in control experiments were age matched to their experimental counterparts. Mice were bred and maintained under specific-pathogen-free conditions in compliance with established ethical guidelines. Animal experimental procedures were approved by the Institutional Animal Care and Use Committee at the Johns Hopkins University.

2.2 | Single-cell RNA-sequencing data analysis

The mouse OE single-cell RNAseq data utilized in this study were publicly available (GSE169011).[18] Briefly, olfactory epithelial single-cell suspensions were prepared from adult mice, sequencing libraries were prepared using 10X Genomics, and libraries were sequenced using Illumina instruments in accordance with manufacturer instructions. Cell type annotations were submitted by the data contributors. A subset of the data was generated from olfactory epithelial cell types. Downstream data analysis and visualization was performed using Seurat v4.0.3[19] and R version 4.0.3(R Foundation, Vienna, Austria).

2.3 | Histochemistry

Animals were anesthetized and transcardially perfused with PBS and 4% paraformaldehyde (PFA). The whole nasal cavity with attached cribriform plate was dissected out and post-fixed in 4% PFA on ice for 1 h with gentle rotation. After being washed in PBS, tissues were equilibrated sequentially in 15% and 30% sucrose. The tissue was then embedded in Optimum Cutting Temperature (OCT, Tissue-Tek, Torrance, CA, USA) for sectioning, and 12-μm frozen sections were processed from cribriform plate side. Staining of tissue sections was performed with hematoxylin and eosin, Giemsa (32884; Sigma, Saint Louis, MO, USA), and Alcian Blue (TMS-010-C; Millipore, Burlington, MA, USA) after washing slides with distilled water. After staining, sections were dehydrated in alcohol, cleared with xylene, and mounted with DPX mounting medium (Electron Microscopy Science, Hatfield, PA, USA). Sections were viewed and imaged using a Revolve microscope (Echo Laboratories; San Diego, CA, USA).

2.4 | Immunohistochemistry

Twelve-micron cryosections were washed in 1x PBS and then blocked in 10% normal serum containing 0.1% Triton X-100, followed by incubation with primary antibodies at 4°C overnight. After washing in PBS, the tissue sections were incubated with Alexa fluor-conjugated secondary antibodies along with Hoescht for nuclear counterstaining. The following primary antibodies were used: chicken anti-Krt5(1:500, 905903; BioLegend, San Diego, CA, USA), rabbit anti-Ki67(1:500, Ab16667; Abcam, Waltham, MA, USA), mouse anti Ki67(1:100, 550609, BD Biosciences, Franklin Lake, NJ, USA), goat anti-CD45(1:250, AF114; R&D, Minneapolis, MN, USA), (1:500, AF3626; R&D, Minneapolis, MN, USA), rabbit anti-Ym-1+Ym-2(1:200, ab211621; Abcam, Waltham, MA, USA); rat anti-CD68(1:200, 137001; BioLegend, San Diego, CA, USA), mouse anti Tuj1(1:300, BioLegend, 801203, San Diego, CA, USA), rabbit anti-ΔNP63(1:1000, 619001; BioLegend, San Diego, CA, USA), mouse anti-EMBP (1:50, sc-365701; Santa Cruz, Dallas, Texas), and rabbit anti-UCH-L1/PGP9.5(1:200, NB300–675; Novus, Centennial, CO, USA). The anti-OST is a guinea pig polyclonal antibody generated against a 16-amino-acid peptide corresponding to the C-terminal residue (YRKKMAGSTITFRTEI) of mouse olfactory sulfotransferase (OST). The specificity of this antibody was verified by the overlap in the staining pattern and the OST mRNA expression determined by in situ hybridization (R Reed, unpublished data).

2.5 | Confocal imaging

Fluorescent immunostaining images were obtained using a Zeiss LSM 780 confocal microscope. CD45 immunostaining was quantified in uniform anatomic locations of the 4E turbinates,[20] using mean gray-scale intensity per area of the lamina propria, and processed with open-source ImageJ software. The average mean grey intensity of immunofluorescence in three separate 4E turbinate coronal sections was calculated in three control and three IL-13 transgenic mice and plotted with standard error of the mean.

2.6 | ELISA

Mouse nasal lavage was performed with 500 μl 1x PBS prior to perfusion and subsequently 100 μl of lavage was added to ELISA plate. The protocol provided with the ELISA kit was followed (cat. no. DY413; R&D Systems, Minneapolis, MN, USA). The OD value was measured at 450 nm using a Thermo Original Multiskan EX plate reader (ThermoFisher, Waltham, MA, USA), and the concentration was calculated using a standard curve.

2.7 | Quantitative PCR

Total RNA was isolated from mouse olfactory tissue using Direct-zol RNA MiniPrep (Zymo Research, Irvine, CA, USA). Equal amounts of RNA were transcribed into cDNA by a high-capacity cDNA reverse transcription kit (Applied Biosystems ref 4368814, Waltham, MA, USA). Ten nanograms of cDNA were added to a 20-μl PCR reaction using TaqMan Fast Universal PCR Master Mix (Applied Biosystems, Waltham, MA, USA) and analyzed on a StepOne Plus System (Applied Biosystems). Initial degeneration was at 95°C for 20 s, followed by 40 cycles of 95°C for 1 s and 60°C for 20 s. Postamplification melting curve analysis was performed to monitor unspecific products. Fold change in mRNA expression

was calculated using the comparative cycle method (2−ΔΔCt). TaqMan probes purchased from Life Technologies Corp (Carlsbad, CA, USA) are as follows: Il13 Mm00434204_m1, Chil4 Mm00840870_m1, CCl24 Mm00444701_m1, Muc5ac Mm01276718_m1, Alox15 Mm0050789_m1, Ccl11 Mm00441238_m1, and Rn18s Mm03928990_g1. All qPCR experiments were performed in duplicate. The data are expressed as the mean ± standard error (SEM). Statistically significant differences between control and olfactory IL-13 mice were analyzed using an unpaired Student's *t*-test (GraphPad Prism v5; GraphPad Software, San Diego, CA, USA).

3 | RESULTS

3.1 | Temporally controlled, olfactory-specific expression of IL-13

The mouse model, using a combination of Cre-lox and the Tet-on system was created by breeding three existing strains of mice (Figure 1A and B). The OMP-Cre mouse line expresses Cre recombinase in mature olfactory neurons. The ROSA26-floxed rtTA mouse line harbors a reverse tetracycline transactivator that is only expressed after Cre-mediated excision of flanking LoxP sites. The third mouse line has a transgene driven by the tet response element (TRE) promoter. We first demonstrated inducible olfactory expression using a TRE-GFP mouse line. We found that the GFP was not expressed in the absence of doxycycline administration but was expressed widely in olfactory neurons after initiating feeding with doxycycline (Figure 1C). We then proceeded to breed in the TRE-IL-13 mouse line to create the final model. In a wild type mouse, no IL-13 can be detected in a nasal lavage fluid, but in the mouse model, IL-13 was consistently present (Figure 1D). Interestingly, DOX induction of olfactory IL-13 appears to have systemic effects, with the mice becoming progressively dehydrated and displaying loss of fur and generalized lethargy. Complete analysis by necropsy did not reveal abnormalities, and specifically eosinophilic inflammation, in any organ system, including skin. The 3-week timepoint after IL-13 induction was chosen for subsequent histopathologic and molecular analysis.

3.2 | IL-4 and IL-13 receptor genes are expressed in non-neuronal olfactory cells

Publicly available single-cell transcriptome profiling data from mouse OE were analyzed to determine which cell types within the OE expressed the IL-13 receptor.[18] All of the major cell types were represented in the data set (Figure 2A). The expression of *Il13ra1* was most robust in non-neuronal epithelial cell types (Figure 2B and C), with an overall low level of Il4ra across all cells. In the violin plots, each individual cell is represented as a black dot, and a colored violin is plotted when there is an appreciable proportion of cells with nonzero expression. In Figure 2(B), sustentacular cells and OSNs have the most black dots because they are the most highly represented cell types in this data set, but there is no colored violin to indicate that a significant proportion of cells express nonzero levels of Il4ra. In Figure 2(C), there are three populations of cells that have colored violins: Bowmans's glands, sustentacular cells, and microvillar cells, suggesting that an appreciable proportion of these cells have nonzero Il13ra1expression.

3.3 | Olfactory expression of IL-13 results in significant neuroepithelial morphologic alterations

The histology of the OE in the mouse model was strikingly changed by IL-13 expression. In particular, there were regions of the OE that became aneuronal, with enlarged sustentacular cells filling the space with a grossly normal epithelial height above the basement membrane (Figure 3A). Other regions appeared to be unaffected and displayed a normal density of neurons. The horizontal basal cells (HBCs), which are normally quiescent cells with a flattened shape, display altered morphology, taking on a rounded or pyramidal shape (Figure 3A and B). This appearance has been described in mitotically active HBCs,[21,22] and we have observed a similar morphologic change in HBCs activated immunologically by TNF-induced inflammation.[23] In the mouse model, pyramidal HBCs are particularly visible in areas of increased neuronal loss, but also in areas that seem otherwise unaffected. An inflammatory cell infiltrate is prominent, with a component of macrophages (Figure 3B). There is an approximately threefold increase in CD45+ cells in the lamina propria in the IL-13-expressing mouse relative to mice not administered doxycycline (Figure 3C and D). In addition to the change in morphology, HBCs are proliferatively active, demonstrated by colocalization of the HBC marker Krt5 with Ki67, a marker of cell division (Figure 4A and B). The aneuronal areas of the epithelium are not due to expanded neurons, as indicated by the absence of nuclei and by PGP9.5 staining of normal-appearing neurons (Figure 4C). Staining for OST shows that sustentacular cell bodies occupy the aneuronal spaces (Figure 4D). The expression of p63, a transcription factor proposed to be the “master regulator” of HBC quiescence, is downregulated as the Krt+ progenitor cells undergo activation (Figure 4E), although some p63+ cells are Ki67+, demonstrating that HBCs are proliferative.

3.4 | Olfactory expression of IL-13 results in high expression of multiple type 2 mediators

Quantitative real-time PCR was used to assess differentially expressed genes induced by IL-13 in olfactory mucosa. Increased mRNA for eotaxins (*Ccl11* and *Ccl24*[24]) as well as *Muc5AC* (encodes mucin[25]), *Alox15* (encodes a promoter of eosinophilic inflammation[26]), and *chil4* (encodes the chitinase Ym2, which is linked to neuroepithelial regeneration[27]) was observed relative to non-doxycycline-treated controls (Figure 5). Expression of *chil4* was particularly elevated, over 900-fold the baseline mRNA level.

3.5 | IL-13 induces mucus production and mild eosinophilic infiltrate

Consistent with the expression of *MUC5AC*, Alcian Blue staining demonstrated increased mucin in the Bowman glands as well as thick mucin filling the adjacent nasal lumen (Figure 6A). Despite the induction of eosinophil chemokine mRNA, Giemsa staining revealed only a modest eosinophilic infiltrate, most prominently near areas of transition between olfactory and respiratory epithelium (Figure 6B).

3.6 | Olfactory expression of IL-13 results in massive expression of the chitinase Ym2, with crystal-like deposits in the mucus

Immunostaining for Ym2 protein is sparse in uninduced mice but is robust in in the setting of IL-13 expression (Figure 7A and B). The staining is most intense in areas of neuronal loss, as well as in mucus in the nasal lumen. Histologic examination demonstrates crystal-

like aggregates extruding from the OE, consistent with the location of Ym2 immunostaining (Figure 7C and D).

4 | DISCUSSION

This study aimed to explore the impact of the type 2 allergic response on olfactory dysfunction. In an inducible model in which doxycycline administration leads to IL-13 expression in mature olfactory neurons, we show significant histological changes in the OE after IL-13 induction. Most notably, neurons became absent in several regions of the OE and there was abundant mucus secretion. The cellular infiltrate appeared macrophage dominant, with unexpectedly low numbers of eosinophils. HBCs were activated and showed increased proliferation as measured by Ki-67 staining after IL-13 induction. Increased expression of *MUC5AC* (encoding mucin) and eosinophil chemokines was observed, as well as *chil4* mRNA and the protein it encodes, Ym2, a chitinase implicated in promoting neuronal regeneration.[27]

By and large, these results are consistent with the reported effect of type 2 inflammation on the OE in mouse models of allergy. Prior models have induced olfactory loss through intranasal allergen challenge.[28,29] These published studies have shown lymphocytic and neutrophilic infiltrates,[29] olfactory epithelial remodeling,[28–30] increased levels of IL-4, IL-5, and IL-13 in the OE,[31,32] and impaired olfactory neurogenesis.[30,31] Prolonged expression of TNF-α by olfactory sustentacular cells in an inducible mouse model observed OSN apoptosis and inhibited regeneration tied to chronic non-type 2 inflammation.[33]

Human histological studies of type 2 inflammation in CRS have shown a complex inflammatory infiltrate throughout the OE.[1,5,6] How this infiltrate may affect olfaction, however, is still a matter of debate. Corticosteroid therapy in CRSwNP has long been known to improve olfaction,[10] and the presumption has been that the mechanism involves primarily reduction of epithelial inflammation. Monoclonal antibodies directed against type 2 inflammatory pathways also can reverse olfactory dysfunction in CRSwNP. Mepolizumab[15] and benralizumab,[14] which block IL-5, and omalizumab,[16] which blocks IgE, have been shown to modestly improve olfaction in CRSwNP patients. Dupilumab, which blocks IL-4/IL-13 receptor signaling, is particularly effective.[13] That this improvement in olfaction happens sooner than polyp reduction or other symptoms suggests that IL-4/IL-13 receptor signaling may directly mediate olfactory loss. Importantly, studies of type 2 cytokines isolated from the olfactory cleft of CRS patients[7,9] show elevated levels of IL-13 but not IL-4, supporting the hypothesis that IL-13 is the key mediator affecting olfaction in type 2 inflammation.

Interleukin-13 may be able to exert this effect on the OE through several avenues, including the Ym2 chitinase, mucus production from Bowman glands, and changes in the barrier function of the olfactory neuroepithelium. First, we have shown in this paper that IL-13 induction increases activation of *chil4*, which encodes for Ym2. Ym2 is a lectin-binding chitinase protein that has been shown to be upregulated in sustentacular cells of the OE after injury to the OE,[27] and overexpression of Ym2 leads to faster regeneration of the OE. In a model of bronchial allergy, Ym2 expression was found to be dependent

on IL-4 and IL-13 signal transduction.[34] Consistent with the non-neuronal expression pattern of the IL-13 receptor, Ym2 expression in the OE appears to be localized to the sustentacular cells. As sustentacular cells play a critical role supporting olfactory neurons, the consequence of IL-13 signaling in these cells may have significant impacts on homeostasis and olfactory function. In neuroimmunologic mouse models, IL-13 has been shown to modulate microglia[35] and has neuroimmunologic activity resulting in functional changes, with IL-13 administration linked with improved mouse task performance after TBI and increased microglial/macrophage phagocytosis of damaged neurons.[36] It could be that IL-13 acts through Ym2 to regulate sustentacular cell activity in the face of olfactory neuron death as part of an effort to promote neurogenesis and epithelial recovery.

Interleukin-13′s effects on mucus production could be another route affecting olfactory function. We show increases in Bowman gland mucin and upregulation of *MUC5AC*, the gene encoding mucin in this inducible mouse model after IL-13 induction. The link between IL-13 and mucus production has been shown extensively in other parts of the airway. IL-13 has been shown to modulate mucus production in human bronchial respiratory epithelium[37] and is known to drive goblet cell hyperplasia in the lung.[38,39] The conductive model of olfactory loss in CRS puts forward obstructive mechanisms that prevent odorants from reaching the olfactory neurons in the first place,[4] and increased volumes of mucus stimulated by IL-13 could impair diffusion of olfactants.[40] IL-13-driven changes in mucus production could affect not only the volume of mucus produced, but also the mucus microenvironment itself, hindering odorant transduction.

Although not directly addressed in this study, epithelial barrier dysfunction represents another potential mechanism by which IL-13 may lead to olfactory loss. Respiratory epithelial cell barrier maintenance genes are known to be often dysregulated in CRS,[41] possibly related to a reduction in airway epithelial cell diversity resulting from IL-13 exposure.[42] Decreased expression of occludin, claudin-3, and ZO-1 have been described in CRSwNP biopsy specimens and in vitro IL-13-treated human nasal epithelial cells, suggesting effects on tight-junction proteins[43]. Barrier function of the OE is largely unstudied, but tight junctions have been shown between neurons and sustentacular cells in rodent olfactory cleft.[44] Alterations in tight junctions in sustentacular cells as a result of IL-13 signaling, or type 2 inflammation more broadly, could potentially affect neuronal survival and function.

The olfactory neuroepithelium represents a unique anatomic niche within the upper airway, having coexisting elements of respiratory mucosa and neural tissue. HBCs are simultaneously a reserve stem cell population for non-neuronal sustentacular cells and for neuronal progenitors. The downregulation of p63 in activated Krt5+ HBCs in our model is consistent with previous work showing p63 downregulation in association with HBC proliferative responses to damage by the olfactotoxins methyl bromide[45] and methimazole.[46] It is possible that the p63-Krt5+ cells reflect a transitory progenitor cell state, as suggested by single-cell RNAseq studies during active regeneration.[47,48] Future pseudotime analyses of scRNAseq data in our model, complemented by fate-mapping studies, may bring regeneration dynamics into better focus. It is clear from our data that in regions of aneuronal mucosa, IL-13 results in HBC morphologic changes associated with activation, but without

sufficient differentiation to maintain a mature neuronal population, at least at the time point studied here.

While this IL-13 expression model provides novel insights, there are important limitations to consider. First, IL-13 alone cannot fully model the cytokine and inflammatory cell milieu in the OE in CRSwNP or the environmental influences underlying disease pathogenesis. Additionally, compared with human CRS, the inducible mouse model of IL-13 produces a greater amount of the cytokine than would be present endogenously, and from a different cellular source. The concentration of IL-13 in the nasal lavage was 2–2.5 times higher than what has been previously reported in allergen challenge murine models of allergic rhinitis.[49] The time course of IL-13 exposure is also certainly significantly longer in human CRSwNP. Further work with this model will seek to correlate findings with the human CRSwNP olfactory mucosa and extend the time course of IL-13 exposure. Electrophysiological and behavioral assessments of olfaction in this model will elucidate the functional importance of these histopathologic and molecular findings.

5 | CONCLUSION

Chronic expression of IL-13 has striking effects on the mouse OE, including regional neuronal loss, HBC activation, mucin production, and inflammatory cell infiltration. While the mechanism of olfactory loss in CRSwNP is unknown, IL-13 appears to have direct impacts on non-neuronal cells in mice that may secondarily alter neuronal function, including a potential role for sustentacular cell-derived Ym2. This mouse model provides an opportunity to elucidate mechanisms of IL-13 effects on the OE, with implications for discovery of novel therapeutic targets for human olfactory dysfunction.

ACKNOWLEDGEMENTS

National Institute for Deafness and Communication Disorders (2T32DC000027 and R01 DC016106) and National Institute of Allergy and Infectious Diseases (R01 AI072502).

Funding information

National Institute on Deafness and Other Communication Disorders, Grant/Award Numbers: 2T32DC000027, R01 DC016106; National Institute of Allergy and Infectious Diseases, Grant/Award Number: R01 AI072502

REFERENCES

1. Kern RC. Candidate’s thesis: chronic sinusitis and anosmia: pathologic changes in the olfactory mucosa. The Laryngoscope. 2000;110(7):1071–1077. [PubMed: 10892672]
2. Kohli P, Naik AN, Harruff EE, Nguyen SA, Schlosser RJ, Soler ZM. The prevalence of olfactory dysfunction in chronic rhinosinusitis. Laryngoscope. 2017;127(2):309–320. [PubMed: 27873345]
3. Smith TD, Bhatnagar KP. Chapter 2 - Anatomy of the olfactory system. In: Doty RL, ed. Handbook of Clinical Neurology. Elsevier; 2019:17–28.
4. Mann NM, Lafreniere D. Anosmia and nasal sinus disease. Otolaryngol Clin North Am. 2004;37(2):289–300. [PubMed: 15064063]
5. Yee KK, Pribitkin EA, Cowart BJ, et al. Neuropathology of the olfactory mucosa in chronic rhinosinusitis. Am J Rhinol Allergy. 2010;24(2):110–120. [PubMed: 20021743]
6. Yee KK, Pribitkin EA, Cowart BJ, Rosen D, Feng P, Rawson NE. Analysis of the olfactory mucosa in chronic rhinosinusitis. Ann N Y Acad Sci. 2009;1170:590–595.. [PubMed: 19686198]

7. Soler ZM, Yoo F, Schlosser RJ, et al. Correlation of mucus inflammatory proteins and olfaction in chronic rhinosinusitis. Int Forum Allergy Rhinol. 2020;10(3):343–355. [PubMed: 31856395]
8. Schlosser RJ, Mulligan JK, Hyer JM, Karnezis TT, Gudis DA, Soler ZM. Mucous cytokine levels in chronic rhinosinusitis-associated olfactory loss. JAMA Otolaryngol– Head Neck Surg. 2016;142(8):731–737. [PubMed: 27228459]
9. Wu J, Chandra RK, Li P, Hull BP, Turner JH. Olfactory and middle meatal cytokine levels correlate with olfactory function in chronic rhinosinusitis. The Laryngoscope. 2018;128(9):E304–E310. [PubMed: 29417576]
10. Stevens MH. Steroid-dependent anosmia. The Laryngoscope. 2001;111(2):200–203. [PubMed: 11210860]
11. Bachert C, Han JK, Desrosiers M, et al. Efficacy and safety of dupilumab in patients with severe chronic rhinosinusitis with nasal polyps (LIBERTY NP SINUS-24 and LIBERTY NP SINUS-52): results from two multicentre, randomised, double-blind, placebo-controlled, parallel-group phase 3 trials. Lancet. 2019;394(10209):1638–1650. [PubMed: 31543428]
12. Bachert C, Mannent L, Naclerio RM, et al. Effect of subcutaneous dupilumab on nasal polyp burden in patients with chronic sinusitis and nasal polyposis: a randomized clinical trial. JAMA. 2016;315(5):469–479. [PubMed: 26836729]
13. Naclerio RM, Hamilos DL, Ferguson BJ, et al. Dupilumab improves sense of smell and reduces anosmia among patients with nasal polyposis and chronic sinusitis: results from a phase 2a Trial. J Allergy Clin Immunol. 2017;139(2):AB90.
14. Bachert C, Han JK, Desrosiers MY, et al. Efficacy and safety of benralizumab in chronic rhinosinusitis with nasal polyps: a randomized, placebo-controlled trial. J Allergy Clin Immunol. 2022;149(4):1309–1317. [PubMed: 34599979]
15. Cavaliere C, Incorvaia C, Frati F, et al. Recovery of smell sense loss by mepolizumab in a patient allergic to Dermatophagoides and affected by chronic rhinosinusitis with nasal polyps. Clin Mol Allergy. 2019;17(1):3. [PubMed: 30804712]
16. Gevaert P, Saenz R, Corren J, et al. Long-term efficacy and safety of omalizumab for nasal polyposis in an open-label extension study. J Allergy Clin Immunol. 2022;149(3):957–965.e3. [PubMed: 34530020]
17. Zheng T, Oh MH, Oh SY, Schroeder JT, Glick AB, Zhu Z. Transgenic expression of interleukin-13 in the skin induces a pruritic dermatitis and skin remodeling. J Invest Dermatol. 2009;129(3):742–751. [PubMed: 18830273]
18. Wang IH, Murray E, Andrews G, et al. Spatial transcriptomic reconstruction of the mouse olfactory glomerular map suggests principles of odor processing. Nat Neurosci. 2022;25(4):484–492. [PubMed: 35314823]
19. Hao Y, Hao S, Andersen-Nissen E, et al. Integrated analysis of multimodal single-cell data. Cell. 2021;184(13):3573–3587. [PubMed: 34062119]
20. Harkema JR, Carey SA, Wagner JG. The nose revisited: a brief review of the comparative structure, function, and toxicologic pathology of the nasal epithelium. Toxicol Pathol. 2006;34(3):252–269. [PubMed: 16698724]
21. Carter LA, MacDonald JL, Roskams AJ. Olfactory horizontal basal cells demonstrate a conserved multipotent progenitor phenotype. J Neurosci Off J Soc Neurosci. 2004;24(25):5670–5683.
22. Brann JH, Ellis DP, Ku BS, Spinazzi EF, Firestein S. Injury in aged animals robustly activates quiescent olfactory neural stem cells. Front Neurosci. 2015;9:367. [PubMed: 26500487]
23. Chen M, Reed RR, Lane AP. Chronic inflammation directs an olfactory stem cell functional switch from neuroregeneration to immune defense. Cell Stem Cell. 2019;25(4):501–513.e5. [PubMed: 31523027]
24. Kagami S, Kakinuma T, Saeki H, et al. Significant elevation of serum levels of eotaxin-3/CCL26, but not of eotaxin-2/CCL24, in patients with atopic dermatitis: serum eotaxin-3/CCL26 levels reflect the disease activity of atopic dermatitis. Clin Exp Immunol. 2003;134(2):309–313. [PubMed: 14616792]
25. Pigny P, Guyonnet-Duperat V, Hill AS, et al. Human mucin genes assigned to 11p15.5: identification and organization of a cluster of genes. Genomics. 1996;38(3):340–352. [PubMed: 8975711]

26. Ivanov I, Kuhn H, Heydeck D. Structural and functional biology of arachidonic acid 15-lipoxygenase-1 (ALOX15). Gene. 2015;573(1):1–32. [PubMed: 26216303]
27. Wang L, Ren W, Li X, et al. Chitinase-like protein Ym2 (Chil4) regulates regeneration of the olfactory epithelium via interaction with inflammation. J Neurosci. 2021;41(26):5620–5637. [PubMed: 34016714]
28. Ozaki S, Toida K, Suzuki M, et al. Impaired olfactory function in mice with allergic rhinitis. Auris Nasus Larynx. 2010;37(5):575–583. [PubMed: 20346605]
29. Liang C, Yang Z, Zou Q, Zhou M, Liu H, Fan J. Construction of an irreversible allergic rhinitis-induced olfactory loss mouse model. Biochem Biophys Res Commun. 2019;513(3):635–641. [PubMed: 30981508]
30. Ueha R, Ueha S, Kondo K, Nishijima H, Yamasoba T. Effects of cigarette smoke on the nasal respiratory and olfactory mucosa in allergic rhinitis mice. Front Neurosci. 2020;14:126. [PubMed: 32132898]
31. Rouyar A, Classe M, Gorski R, et al. Type 2/Th2-driven inflammation impairs olfactory sensory neurogenesis in mouse chronic rhinosinusitis model. Allergy. 2019;74(3):549–559. [PubMed: 29987849]
32. Hussain I, Randolph D, Brody SL, et al. Induction, distribution and modulation of upper airway allergic inflammation in mice. Clin Exp Allergy. 2001;31(7):1048–1059. [PubMed: 11467996]
33. Victores AJ, Chen M, Smith A, Lane AP. Olfactory loss in chronic rhinosinusitis is associated with neuronal activation of c-Jun N-terminal kinase. Int Forum Allergy Rhinol. 2018;8(3):415–420. [PubMed: 29193850]
34. Webb DC, McKenzie ANJ, Foster PS. Expression of the Ym2 lectin-binding protein is dependent on interleukin (IL)-4 and IL-13 signal transduction: identification of a novel allergy-associated protein*. J Biol Chem. 2001;276(45):41969–41976. [PubMed: 11553626]
35. Shin WH, Lee DY, Park KW, et al. Microglia expressing interleukin-13 undergo cell death and contribute to neuronal survival in vivo. Glia. 2004;46(2):142–152. [PubMed: 15042582]
36. Miao W, Zhao Y, Huang Y, et al. IL-13 ameliorates neuroinflammation and promotes functional recovery after traumatic brain injury. J Immunol. 2020;204(6):1486–1498. [PubMed: 32034062]
37. Tanabe T, Fujimoto K, Yasuo M, et al. Modulation of mucus production by interleukin-13 receptor alpha2 in the human airway epithelium. Clin Exp Allergy J Br Soc Allergy Clin Immunol. 2008;38(1):122–134.
38. Finkelman FD, Yang M, Perkins C, et al. Suppressive effect of IL-4 on IL-13-induced genes in mouse lung. J Immunol Baltim Md 1950. 2005;174(8):4630–4638.
39. Wills-Karp M, Luyimbazi J, Xu X, et al. Interleukin-13: central mediator of allergic asthma. Science. 1998;282(5397):2258–2261. [PubMed: 9856949]
40. Hahn I, Scherer PW, Mozell MM. A mass transport model of olfaction. J Theor Biol. 1994;167(2):115–128. [PubMed: 8207942]
41. Richer SL, Truong-Tran AQ, Conley DB, et al. Epithelial genes in chronic rhinosinusitis with and without nasal polyps. Am J Rhinol. 2008;22(3):228–234. [PubMed: 18588753]
42. Ordovas-Montanes J, Dwyer DF, Nyquist SK, et al. Allergic inflammatory memory in human respiratory epithelial progenitor cells. Nature. 2018;560(7720):649–654. [PubMed: 30135581]
43. Huang ZQ, Liu J, Ong HH, et al. Interleukin-13 alters tight junction proteins expression thereby compromising barrier function and dampens rhinovirus induced immune responses in nasal epithelium. Front Cell Dev Biol. 2020;8:572749. [PubMed: 33102478]
44. Steinke A, Meier-Stiegen S, Drenckhahn D, Asan E. Molecular composition of tight and adherens junctions in the rat olfactory epithelium and fila. Histochem Cell Biol. 2008;130(2):339–361. [PubMed: 18523797]
45. Schnittke N, Herrick DB, Lin B, et al. Transcription factor p63 controls the reserve status but not the stemness of horizontal basal cells in the olfactory epithelium. Proc Natl Acad Sci U S A. 2015;112(36):E5068–5077. [PubMed: 26305958]
46. Chen M, Tian S, Yang X, Lane AP, Reed RR, Liu H. Wnt-responsive $Lgr5^{+}$ globose basal cells function as multipotent olfactory epithelium progenitor cells. J Neurosci Off J Soc Neurosci. 2014;34(24):8268–8276.

47. Herrick DB, Lin B, Peterson J, Schnittke N, Schwob JE. Notch1 maintains dormancy of olfactory horizontal basal cells, a reserve neural stem cell. Proc Natl Acad Sci U S A. 2017;114(28):E5589–E5598. [PubMed: 28637720]

48. Fletcher RB, Prasol MS, Estrada J, et al. p63 regulates olfactory stem cell self-renewal and differentiation. Neuron. 2011;72(5):748–759. [PubMed: 22153372]

49. Li J, Wang B, Luo Y, Zhang Q, Bian Y, Wang R. Resveratrol-mediated SIRT1 activation attenuates ovalbumin-induced allergic rhinitis in mice. Mol Immunol. 2020;122:156–162. [PubMed: 32361418]

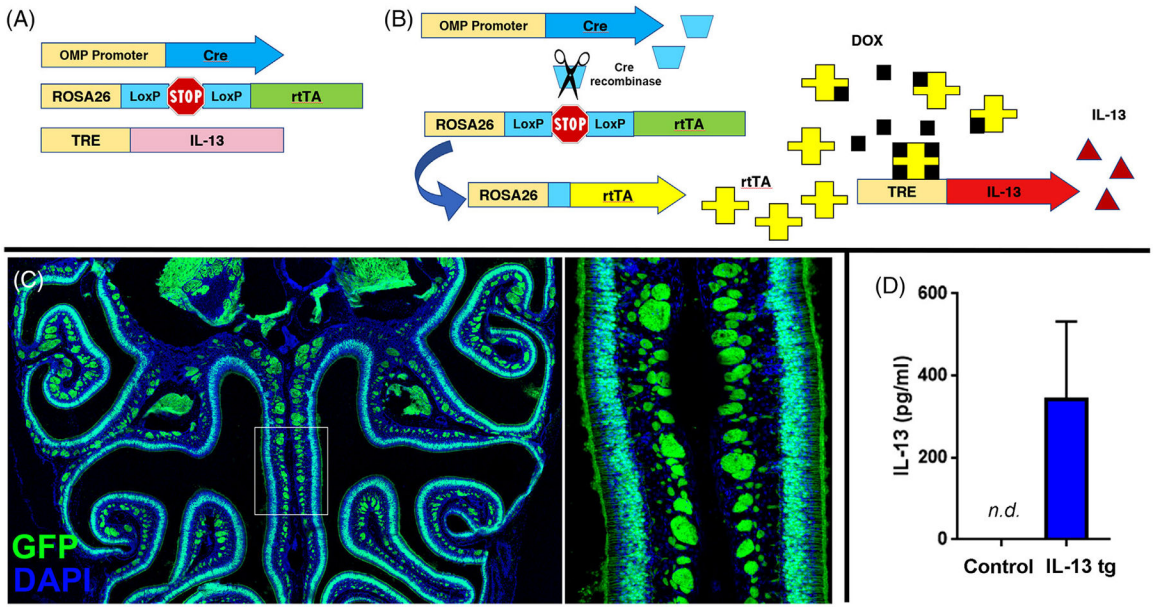

FIGURE 1.

(A) Three genetic constructs combined in mouse model through breeding. (B) Schematic diagram of model mechanism. Cre recombinase driven by the OMP promoter in mature olfactory neurons removes lox-stop, allowing expression of the reverse tetracycline transactivator (rtTA). When doxycycline is administered in the mouse food, rtTA is allosterically activated and can bind the tet-response element (*TRE)* promoter, resulting in IL-13 expression in mature olfactory neurons. (C) Demonstration of specificity of the OMP-cre/ROSA26-rtTA in the olfactory epithelium. Doxycycline induces GFP expression in olfactory neurons, when a mouse line with a TRE-GFP transgene is bred into the model. (D) IL-13 is not expressed in mice not fed doxycycline but is detectable in nasal lavage fluid after doxycycline induction

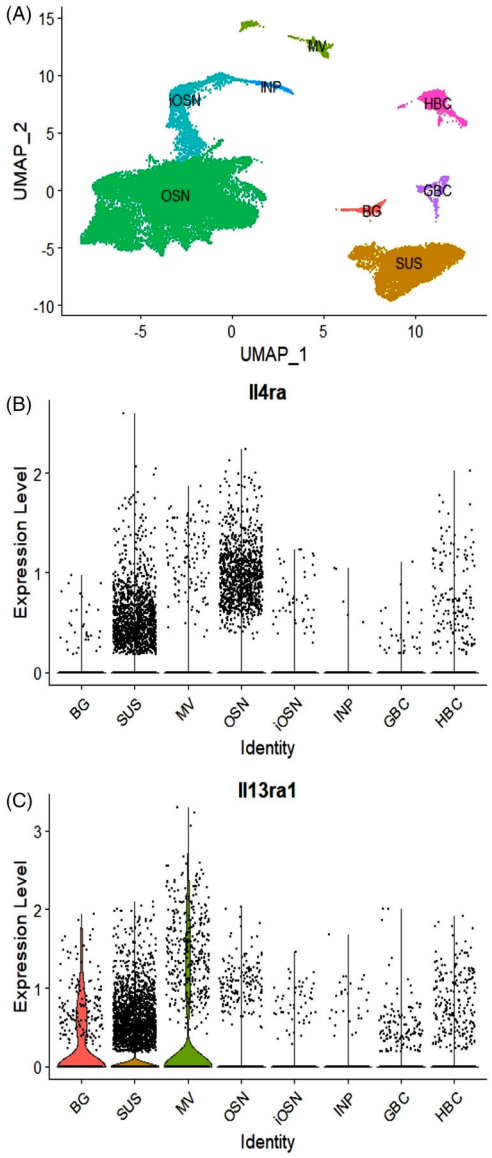

FIGURE 2.

(A) UMAP demonstrating major olfactory epithelial cell types represented in the data. (B) Expression of *Il4ra* (log transformed). The absence of violin plots indicates that there are no cell types in which the majority of captured cells have nonzero expression. Each dot represents an individual cell, with SUS and OSN comprising a large proportion of captured cells in this data set. Cells above the *x*-axis express nonzero levels of IL-4ra1. (C) Expression of Il13ra1 (log transformed). Three non-neuronal cell types—SUS, BG, and MV—have violin plots showing nonzero expression of Il13ra1 in the majority of cells. OSNs do not have a violin plot and have a small number of cells with nonzero expression. Coexpression of both receptor subunits is necessary for a functional IL-13 receptor. BG, Bowman gland; GBC, globose basal cell; HBC, horizontal basal cell; iOSN, immature olfactory sensory neuron; INP, immediate neuronal precursor; MV, microvillar cell; OSN,

olfactory sensory neuron; SUS, sustentacular cell; UMAP, uniform manifold approximation and projection

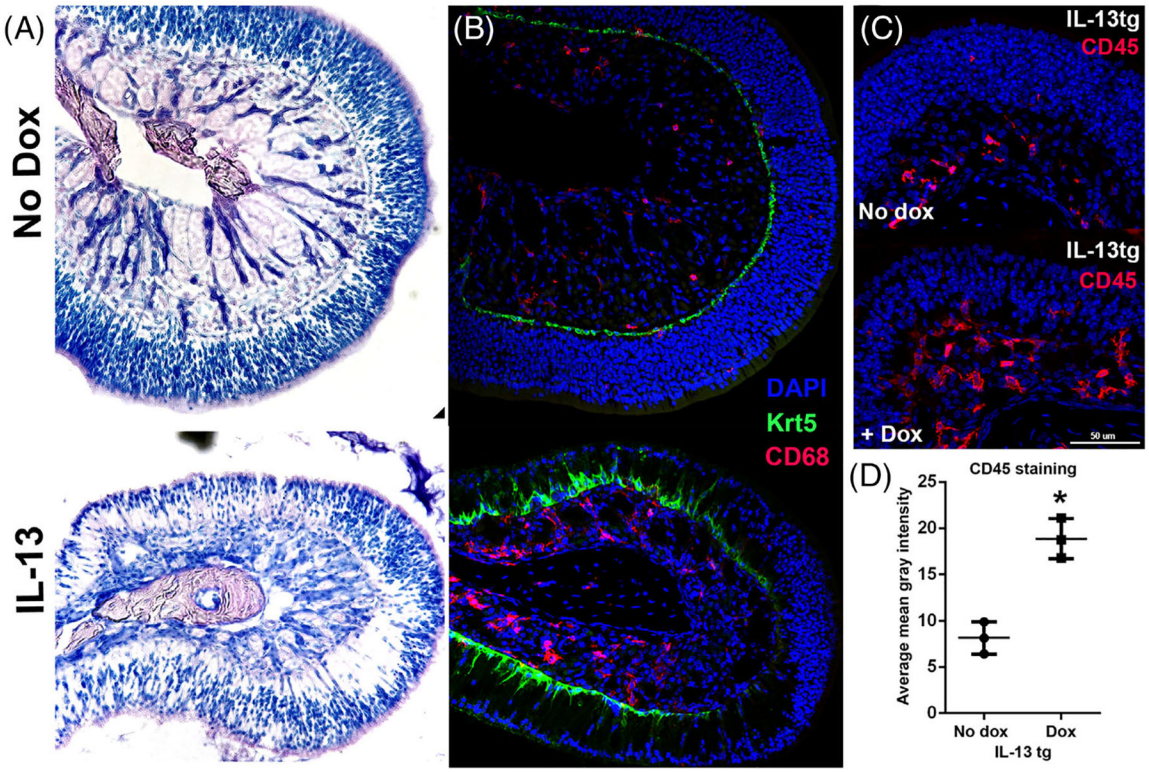

FIGURE 3.

(A) Marked histopathology in the olfactory IL-13 mouse model. Top: normal histology in the absence of doxycycline. Bottom: olfactory turbinate in mouse with IL-13 induction showing regional loss of neurons with maintenance of olfactory thickness. (B) Morphologic change in horizontal basal cells and macrophage infiltrate. Upper image shows normal turbinate in the absence of doxycycline, with flat, quiescent horizontal basal cells (Krt5, green) and few macrophages (CD67, red). Lower image demonstrates pyramidal shape of horizontal basal cells, associated with activation, especially in areas of neuronal loss. Macrophages are prominent in the lamina propria. (C, D) Over twofold increased inflammatory cells in lamina propria in the olfactory IL-13 mice, as quantified by average CD45 staining per tissue area in the lamina propria of turbinate 4E (*$p = 0.007$). $n = 3$ mice per group

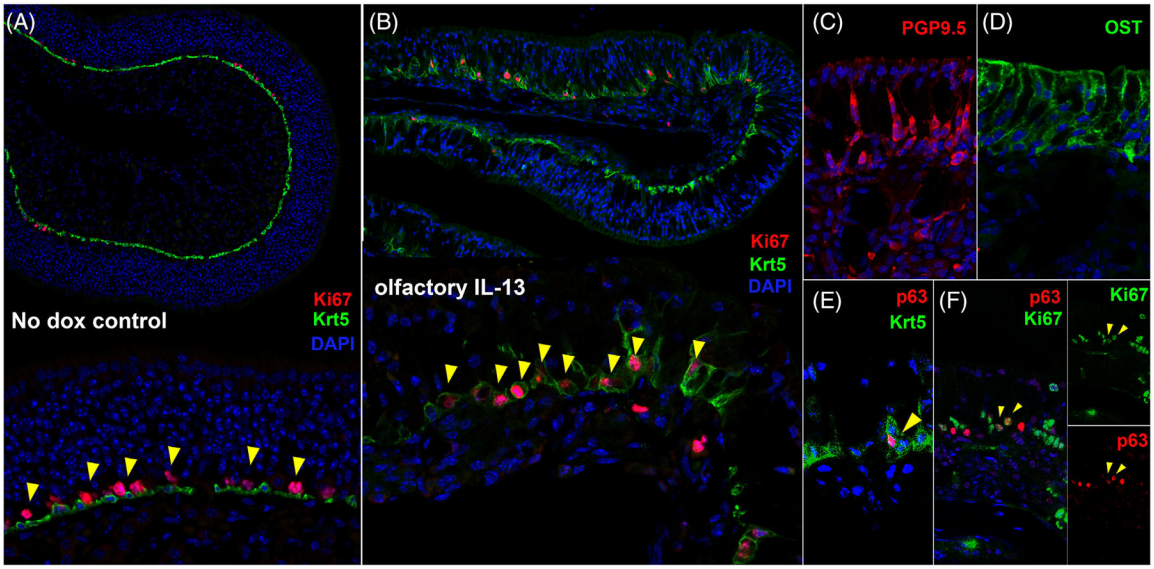

FIGURE 4.

Proliferation of basal progenitor cells in aneuronal regions of the olfactory IL-13 mouse model. (A) In uninduced mice, Ki-67 is localized to dividing globose basal cells that sit just apical to the quiescent Krt5+ horizontal basal cells (HBCs). (B) After IL-13 induction, colocalization of Ki-67 and Krt5 is present, signifying proliferation of Krt5+ basal progenitor cells, consistent with activated HBCs. (C) PGP9.5 staining of olfactory neurons further demonstrates regions that are aneuronal. (D) Immunostaining for the sustentacular cell protein olfactory sulfotransferase (OST) shows expanded sustentacular cells in aneuronal regions. (E) Expression of p63 is downregulated in most activated Krt5+ HBCs. (F) Colocalization of p63 and Ki67 is observed, indicating proliferation of HBCs

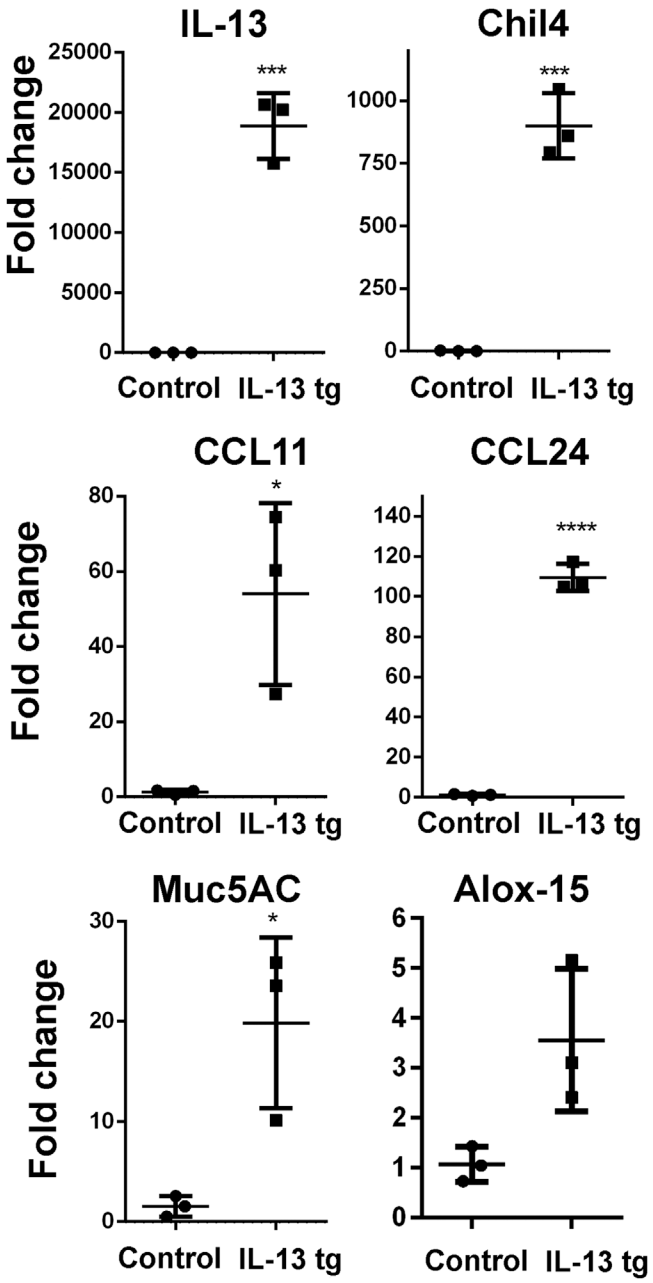

FIGURE 5.

Increased expression of multiple mediators in olfactory IL-13 mouse model. The expression of the IL-13 transgene at high levels is confirmed. Downstream IL-13 effectors identified in mouse respiratory epithelium are induced, including Chil4 (YM2), CCL2 and CCL 24 (eotaxins), Mucin 5 AC, and ALOX15

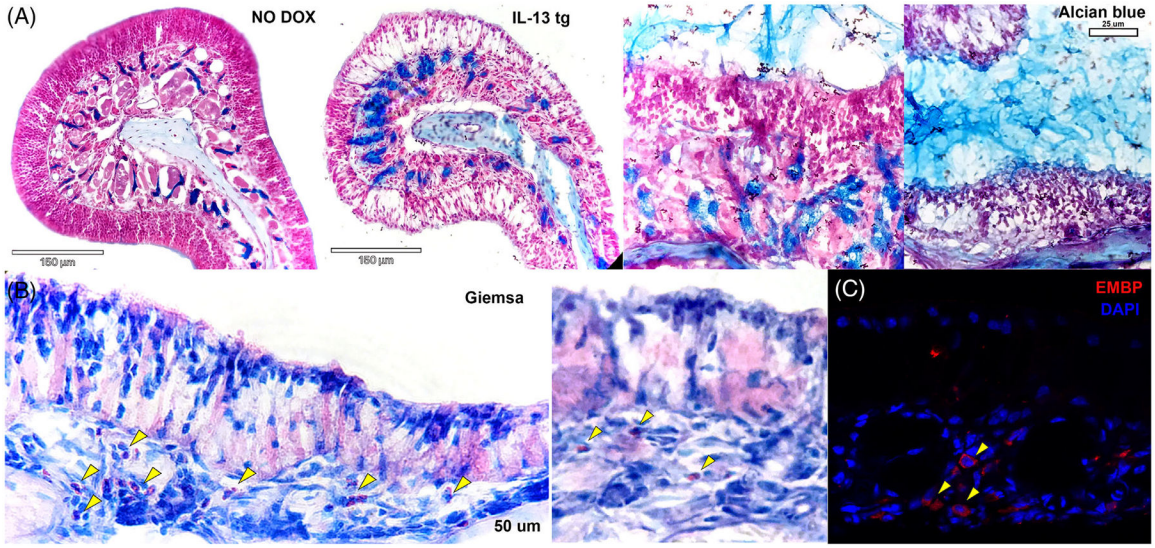

FIGURE 6.

Increased expression of mucus and infiltration of eosinophils in the olfactory IL-13 mouse. (A) Alcian blue staining demonstrates prominent Bowman glands after induction of IL-13 in the mouse model (left side). Abundant mucus is present in the lumen of the olfactory region of the nose (right side). (B) Giemsa staining demonstrates a modest eosinophilic infiltrate in the olfactory epithelium, more prominent in areas of transition to respiratory mucosa (left) but also in the olfactory turbinates (right). Staining for eosinophil major basic protein confirms presence of eosinophils in the turbinates. (C) Immunostaining for eosinophil major basic protein confirms presence of eosinophils in the turbinates. Eosinophils are seen extremely rarely in normal mouse olfactory epithelium

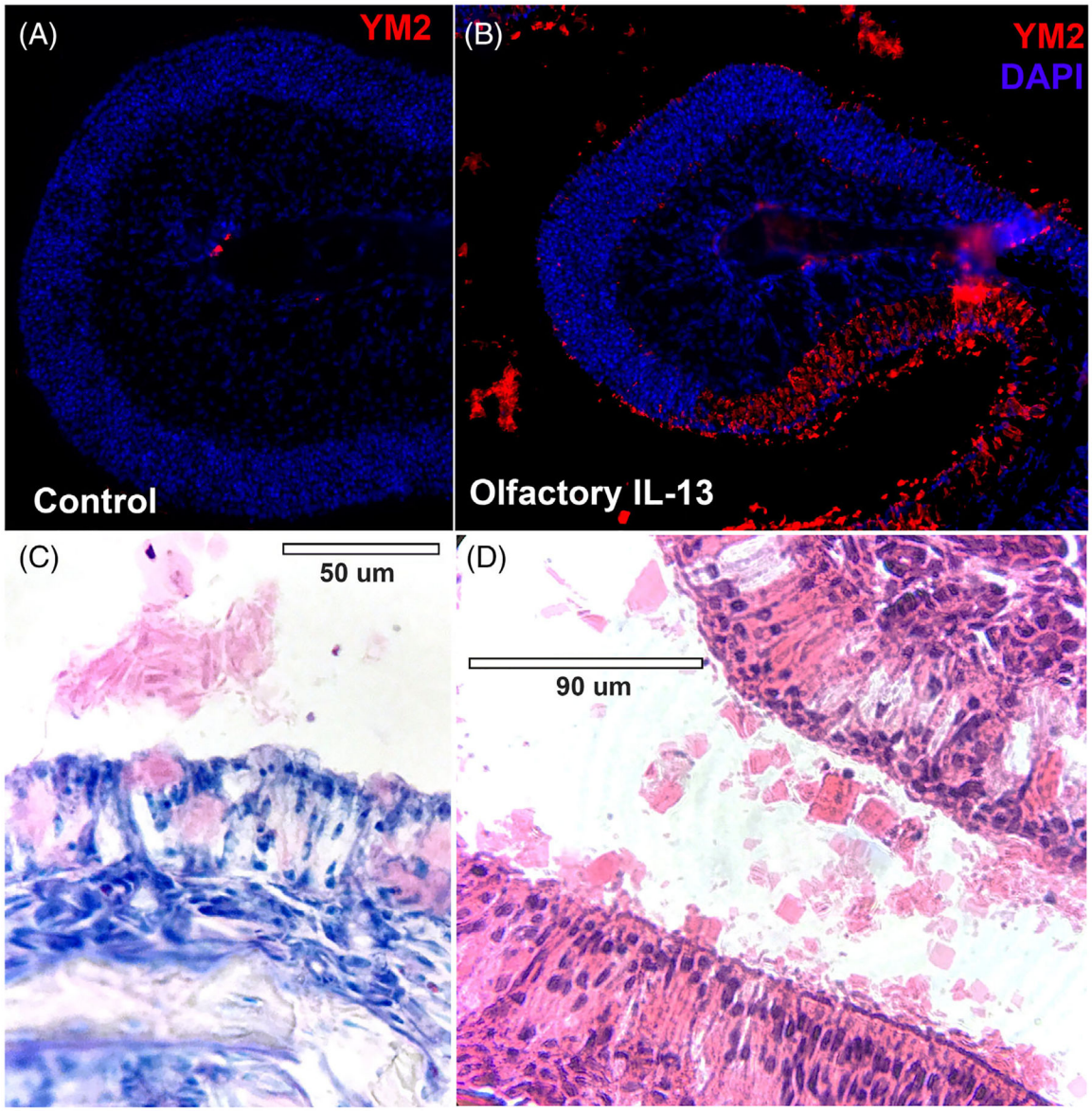

FIGURE 7.

Ym2 protein is expressed in high levels in affected olfactory epithelium, filling sustentacular cell cytoplasm and forming crystals in the mucus. (A, B) Immunohistochemistry showing that Ym2 is expressed at low levels in uninduced olfactory mucosa but is expressed robustly in the olfactory IL-13 model, particularly in areas of neuronal loss. Staining is also seen in the mucus outside of the olfactory tissue. (C, D) Giemsa and H&E staining demonstrate the crystalline material outside of the olfactory mucosa, consistent with location of Ym2 staining